CHAPTER 5

GROUND BASED BISTATIC SCATTEROMETER MEASUREMENT FOR THE ESTIMATION OF GROWTH VARIABLES OF LADYFINGER CROP AT X-BAND

5.1 INTRODUCTION

Agricultural crops play an important role in the economy as well as food security for any country. The reliable and timely information about agricultural crops is necessary for the day-by-day increasing population worldwide. The accurate estimation of crop growth variables is important since it provides information about crop health conditions. The crop stress can be analyzed immediately by the estimation of crop growth variables at the different growth stages. Remote sensing techniques provide a time-saving and influential approach for monitoring and estimating the critical biophysical parameters and characteristics of the agriculture crops. Conventional visible and near-infrared remote-sensing techniques are widely used; however, they have limitations. Microwave remote sensing offers some potential improvements over conventional remote sensing due to its all-weather day-and-night imaging capabilities, penetration into the vegetation canopies, and sensitivity towards dielectric and geometric properties (Kim et al. 2013).

Microwave methods have extensively been used to characterize biophysical crop parameters. Most of this work has been done by relating backscattering coefficients from active microwave methods to observed crop parameters under field conditions. Ground-based polarimetric scatterometer systems are very valuable in establishing basic relationships because both target and system parameters can be well controlled. An important advantage of these systems that can be exploited is the temporal observation of a specific crop target. Several articles have used this approach to explore relationships between backscattering

coefficients and biophysical parameters (Wegmuller 1990; Bouman 1991; Toure et al. 1994; Kim et al. 2013). The results of this investigation offer new information that can be used to monitor and detect different crop growth stages from scatterometer data.

The recent research interest has increased towards the bistatic and multi-static radar measurement for the monitoring of the agricultural crops among the researchers/scientists community working in the field of microwave remote sensing. A few studies are available describing the bistatic scattering behavior of agricultural crops. It is needed to study the scattering response regarding the bistatic scatterometer system and to explore the potential of bistatic radar for the monitoring and estimation of biophysical parameters of agricultural crops

For robust estimation methods, the temporal change of measurements of scattering coefficients at different polarization and incidence angles during the growing season still needs to be documented, together with the temporal change of biophysical parameters. The modeling based on the conventional mathematical tools is not suitable for dealing with ill-defined and uncertain crop canopy structure with the scattering coefficients. A fuzzy inference system, by contrast to conventional modeling, employing fuzzy if-then rules, membership function, and logical operation, can model the qualitative aspects of human knowledge and reasoning processes without employing precise quantitative analyses. This fuzzy modeling or fuzzy identification, first explored systematically by (Takagi and Sugeno 1985), has found several practical applications in prediction and inference (Kandel 1988). However, there are some basic aspects of this approach that are in need of better understanding. There is a need for effective methods for tuning parameters of the membership functions (MF) and consequent function so as to minimize the output error measure or maximize performance index. In this perspective, the aim of this chapter is to use a novel method called Adaptive Neural Network based Fuzzy Inference System, also known

as ANFIS which can serve as a basis for optimizing a set of fuzzy if-then rules with appropriate membership functions and consequent function to find the required input-output values. By integrating the fuzzy inference system into the framework of adaptive neural networks, a neuro-fuzzy algorithm known as ANFIS is obtained, which would be investigated for the estimation of crop growth parameters in this chapter.

The objective of the present study is focused on the investigation of microwave response of crop growth variables and assessment of the subtractive clustering based adaptive neuro-fuzzy inference system (S-ANFIS) for the estimation of ladyfinger crop growth variables. For this purpose, multi-temporal, dual polarized (HH and VV) and multi-angular data sets at X-band were acquired by the ground-based bistatic scatterometer system. In the present chapter, section 5.2 is focused on the discussion of experimental set-up and measurements technique and performance indices, section 5.3 includes the details of S-ANFIS algorithm, section 5.4 explains the results and discussion and section 5.5 contains the concluding remarks of the present investigation.

5.2 EXPERIMENTAL DETAILS

An outdoor crop bed of area 10×10 m^2 was prepared for bistatic scatterometer measurement at different growth stages of ladyfinger crop besides the Department of Physics, IIT (BHU) Varanasi, India. The ladyfinger crop was sown at the spacing of 20 cm between the rows on 4 May 2016 in the measurement site. The bistatic specular scatterometer measurements were carried out from 23 May 2016 with an interval of 10 to 15 days. The bistatic scatterometer measurements of ladyfinger crop were carried out at X-band for HH- and VV-polarizations at six different growth stages. The specifications of the bistatic scatterometer system are summarized in Chapter 2. The crop growth variables were also measured at the time of each bistatic scatterometer measurement. The soil moisture was tried to keep constant during the bistatic scatterometer measurements by irrigating the ladyfinger

crop bed as and when required. The detailed procedure for the measurement of crop growth parameters (FBm, LAI, PH, and VWC) of the ladyfinger crop at its various growth stages is given in Chapter 2. The Equations (2.14) and (2.15) given in Chapter 2 were used for the computation of FBm and VWC, respectively.

5.3 METHODS

5.3.1 Description of S-ANFIS

ANFIS is an integration of fuzzy inference system (FIS) and multi-layer adaptive neural network suggested by (Jang 1993). In fuzzy inference system, the complex system needs a very long time to adjust the parameters of membership function, consequent equation and fuzzy rules. Therefore, adaptive neural network along with fuzzy inference system is used to tune the parameters of membership functions, consequent equation, and fuzzy rules associated with the fuzzy inference system. The subtractive clustering based adaptive neuro-fuzzy inference system (S-ANFIS) is the combined form of two important soft computing algorithms, namely subtractive clustering based fuzzy inference system algorithm and multi-layer adaptive neural network algorithm.

The brief description of the fuzzy inference system and the subtractive clustering based fuzzy inference system are given in Chapter 3 under Section 3. The adaptive artificial neural network is a neural network consisting of layers of parallel processing elements called neurons, characterized by the transfer function with adjustable weight and bias parameters. The adaptive artificial neural network involves the automatic adjustment of synaptic weight and bias parameters of the neuron in accordance with the error signal. The training of the artificial neural network is a process to determine the adjustable parameter so as to fit the training data. The basic back propagation learning algorithm or the least square method is used for the training of the artificial neural network (Drake 2000). A detailed report about the ANFIS can be found in (Jang 1993).

From Figure 5.1**,** it can be seen that the S-ANFIS structure has a five layer. The first layer and fourth layer has an adaptive node while the remaining node has a fixed node. The brief descriptions of each layer are defined as

Layer 1: In this layer, the crisp inputs are fuzzified via the membership function. Here the crisp input signal is fed to the node *i*. The output of each node is the value of membership function that is given by the input of the membership functions which is associated with a linguistic label (fuzzy set). The output can be defined as

$O_{1,i} = \mu_i^k$ for $i=1,2$

Layer 2: The nodes in this layer are fixed or non-adaptive. If it were two input data *x* and *y,* the output of each node would be given by the product of all rules for the two inputs from the first layer.ie.

$O_{2,i} = W_i = \mu_i^k(x) * \mu_i^k(y)$ for $i=1,2$

Where W_i is the output that measures the firing strength of each rule. This layer is known as the membership layer.

Layer 3: In this layer, each node is fixed or non-adaptive. Each node determines the normalized firing strength for each rule. It is defined by the ratio of individual firing strength to the sum of firing strength of all the rules given by the second layer. Therefore, this layer is known as the rule layer. Hence, the output is the normalized firing strength of a given rule and is defines as

$O_{3i} = \overline{W}_i = \frac{W_i}{W_1+W_2}$ for $i=1,2$

Layer 4: In this layer, every node is the adaptive node. It calculates the individual output values 'f_i' from the output of the previous rules. Each individual node of this layer is connected to the respective normalization node in layer 3. Its output is given by

$O_{4,i} = \overline{W}_i f_i = \overline{W}_i (p_i x + r_i)$ for $i=1,2$

Where p_i *and* r_i are consequent parameters of 'f_i'. In this layer, these parameters are adjusted according to the minimum error between the output by the neuro-fuzzy system and desired outputs.

Layer 5: This layer has a single fixed or non-adaptive node. The overall output is calculated as the summation of all input signals from the previous node. The output of this node is defined as

$O_{5,i} = \sum_i \overline{W}\ i\ f_i = \frac{\sum W_i f_i}{\sum W_i}$ for $i=1,2$

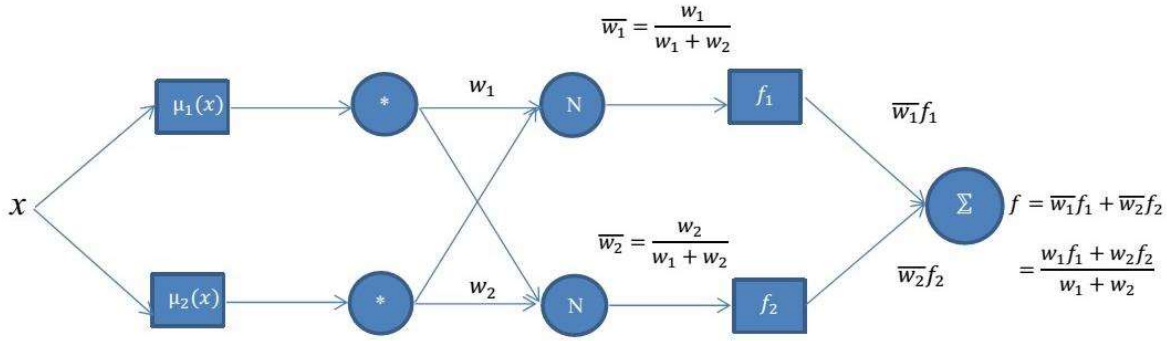

Figure 5.1 Architecture of S-ANFIS

The functions *genfis-2* and *anfis* available in the fuzzy logic toolbox of MATLAB were used for optimizing the crop variable estimation problem using the S-ANFIS algorithm. The final optimized parameters of the S-ANFIS algorithm were determined via an extensive trial-error method. The cluster radius is a very important optimizing parameter ranging from 0 to 1. Since the smaller value of the cluster radius will result in a large number of cluster centers leading to a large number of fuzzy rules, which would lead to overfitting the training data. While the larger value of the cluster radius generates the fewer cluster centers which would lead to the small number of fuzzy rules producing a courser model. Therefore, the optimum value of the cluster radius should be chosen for a good balance between the fuzzy rule and root mean square error due to the higher value of the cluster radius. In the S-ANFIS

algorithm, the optimum value of the cluster radius was chosen by calculating the RMSE between observed and estimated value (Chiu 1994). The optimum value of radii was found by training the model using radii values between 0 and 1 at steps of 0.05 by the trial-error method. The optimum value of the cluster radius was chosen, where the RMSE started to diverge at the training of the S-ANFIS algorithm.

5.4 RESULTS AND DISCUSSION

Figure 5.2 shows the temporal variation of crop growth variables, namely FBm, VWC, LAI, and PH of the ladyfinger crop. All the crop growth variables of ladyfinger crop were found increasing with the age of crop up to 80 days after the sowing of the crop and then decreased slightly. Figures 5.3 and 5.4 show the temporal variation of the specular bistatic scattering coefficient of ladyfinger crop at its different growth stages at HH and VV polarizations, respectively. At both the polarization, the specular bistatic scattering coefficient was found to decrease with the incidence angles and as well as with the age of crop until the maturity of the crop. After the maturity stage of the crop, the specular bistatic scattering coefficient was found to increase slightly.

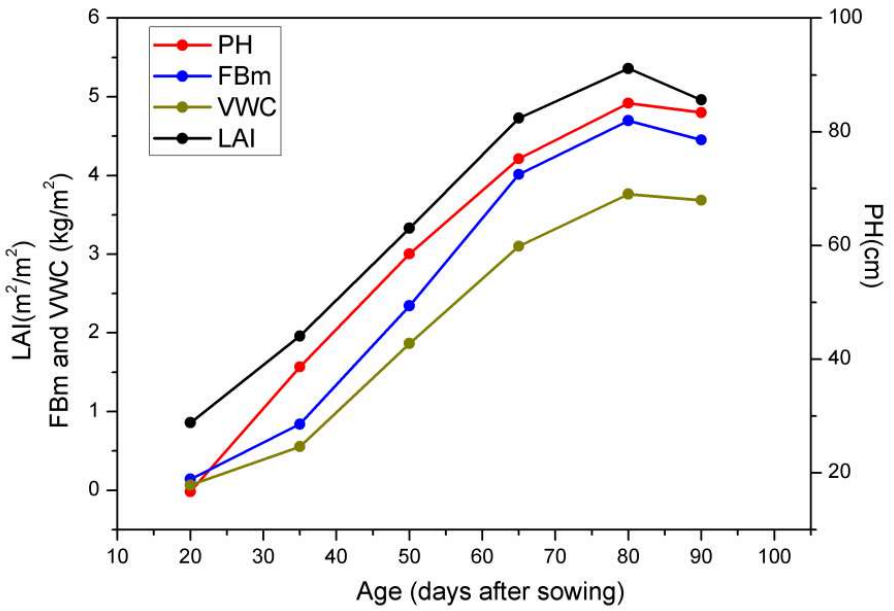

Figure 5.2 Temporal variation of crop growth parameters

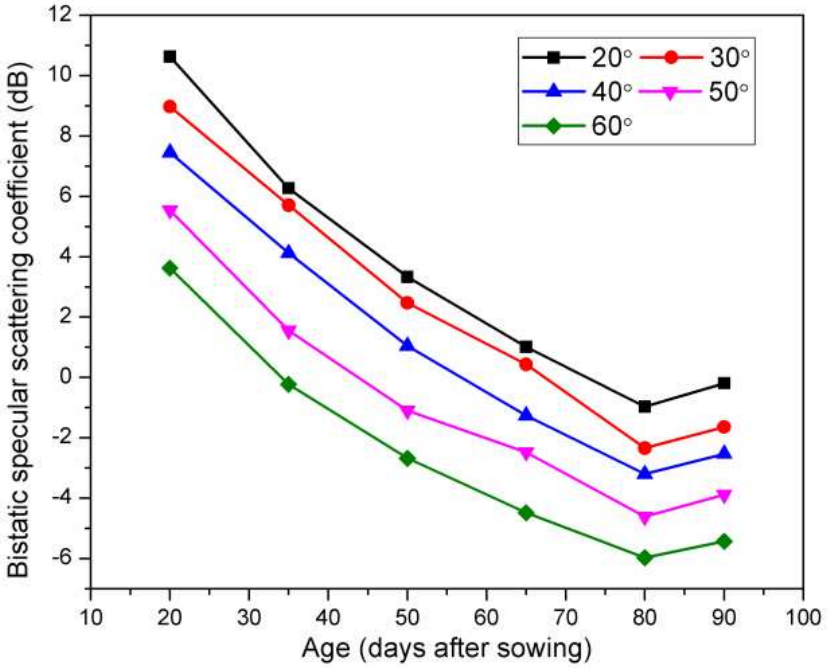

Figure 5.3 Temporal variation of bistatic specular scattering coefficient at X-band for HH-polarization

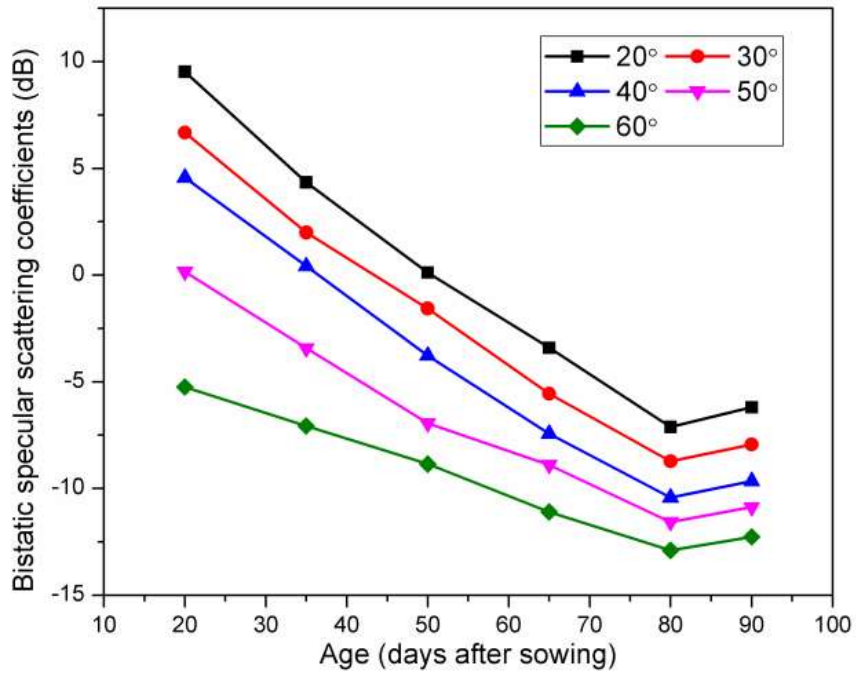

Figure 5.4 Temporal variation of bistatic specular scattering coefficient at X-band for VV-polarization

The variation in the magnitude of the specular bistatic scattering coefficient was found more at early growth stages than the older growth stages of the crop. The main contribution for specular bistatic scattering is the coherent contribution of the incident radiation by the crop beneath soil surface in the specular direction. At the early growth stages of the crop, when the crop growth variables were very small, the attenuation caused to the coherent contribution of the incident radiation by the crop beneath soil surface in the specular direction was low in comparison to the older growth stages. Therefore, the value of the specular bistatic scattering coefficients was found more at the early growth stages than the older growth stages of crop. After the maturity stage, the crop growth variables started to decrease; therefore, the coherent component of the incident radiation by the crop beneath soil surface started to increase again; hence the value of the specular bistatic scattering coefficient was found to increase slightly. At each growth stage of the crop, the magnitude of the specular bistatic scattering coefficient was found to be higher at HH- polarization than VV-polarization. The low value of the specular bistatic scattering coefficient is attributed to higher interaction of the radiation with vertical stalks at VV-polarization than the HH-polarisation. The vertical stalks may be modeled as the vertically oriented lossy dielectric cylinders. Therefore, the magnitude of the scattering coefficient is low at VV- polarization in comparison to HH- polarization (Ulaby et al. 1987). At early growth stage of crop, when crop growth variables were small after 20 days of sowing (FBm = 0.14 kg/m^2, VWC=0.06 kg/m^2 , LAI = 0.86 m^2/m^2 and PH = 16.72 cm), the dynamic range of specular bistatic scattering coefficient was found to be 7.00 dB and 14.77 dB for HH and VV polarization respectively, whereas, after 80 days of sowing, when the crop growth variables were higher (FBm = 4.69 kg/m^2, VWC=3.76 kg/m^2, LAI = 5.35 m^2/m^2 and PH = 85.10 cm), the dynamic range was found to be 5.24 dB and 6.07 dB for HH and VV-polarizations, respectively. Therefore, the temporal trend was found more flat as the crop grows since the effects of soil

were quenched by the developing vegetation. The variation in the dynamic range of the specular bistatic scattering coefficient was found more at VV polarization than at HH polarization. Therefore, the specular bistatic scattering coefficient at VV polarization was more sensitive to the crop growth variables than at HH polarization.

The linear regression analysis was carried out between the specular bistatic scattering coefficients and ladyfinger crop growth variables at all the incidence angles for HH- and VV-polarizations to select the optimum angle of incidence and polarization for the estimation of crop growth variables using S-ANFIS algorithm. The specular bistatic scattering coefficients were found to be highly correlated at 40^{o} incidence angle for both the polarizations. Table 5.1 shows the coefficient of determination (R^2) between the specular bistatic scattering coefficients and different growth variables of ladyfinger crop at both the polarizations for the entire angular range. The coefficients of determination (R^2) were found marginally higher at VV- polarization than HH- polarization at 40^{o} incidence angle. Thus, the data sets (specular bistatic scattering coefficient and crop growth variables) at 40° incidence angle and VV polarization were considered for the estimation of crop growth variables at the X-band. The interpolation of the data sets was done to generate the additional 71 days data sets with the age of crop (20 days to 90 days after sowing) at the interval of one day for the accurate estimation of the crop growth variables. The 54 data sets out of 71 data sets were used for the training of the S-ANFIS. The remaining data sets at the interval of 3 days were used for the testing to assess the generalization capability of the developed S-ANFIS algorithm.

Table 5.1 The values of the coefficient of determination (R^2) between bistatic specular scattering coefficient and crop growth parameters

Incidence angle (degree)	Coefficient of determination (R^2)							
	HH-pol				VV-pol			
	FBm	LAI	PH	VWC	FBm	LAI	PH	VWC
20°	0.926	0.949	0.973	0.929	0.935	0.939	0.968	0.946
30°	0.942	0.946	0.973	0.954	0.952	0.954	0.975	0.959
40°	0.948	0.959	0.978	0.955	0.959	0.959	0.984	0.967
50°	0.900	0.931	0.974	0.905	0.925	0.932	0.966	0.938
60°	0.915	0.946	0.973	0.917	0.945	0.927	0.943	0.958

The specular bistatic scattering coefficients at 40° incidence angle and VV- polarization was taken as input data, and crop growth variables like FBm, LAI, PH, and VWC were taken as output data for the training of developed S-ANFIS algorithm. For the present investigation, the optimum value of the cluster radius was found 0.6 for the accurate estimation of all crop growth variables except the 0.4 for VWC at VV polarization. Figures 5.5-5.8 show the MF curve for different crop growth variables. The different number of cluster has been generated for each data set at VV- polarization.

The performance index RMSE was applied to evaluate the performance of the S-ANFIS algorithm for the estimation of crop growth variables at VV- polarization. The performance indices were computed between observed crop growth variables and S-ANFIS estimated crop growth variables. Tables 5.2 show the calculated values of the RMSE between the estimated and observed crop growth variables for the optimized value of the cluster radius of the S-FIS and S-ANFIS algorithm. The RMSE values between observed and estimated values of the crop parameters showed that the performance of the S-FIS was improved by using the S-FIS combined with the artificial neural network. Figures 5.9-5.12 show the plot between the observed and estimated value of the crop growth parameters. The values of RMSE between

observed and estimated values of the crop growth parameters during the training and testing of the S-ANFIS algorithm are also shown in the same figures. The values of estimated and observed crop growth variables were found almost close during the testing of the S-ANFIS algorithm. The performance of the S-ANFIS algorithm for the estimation of crop growth variable at VV- polarization was found good during the testing of data sets.

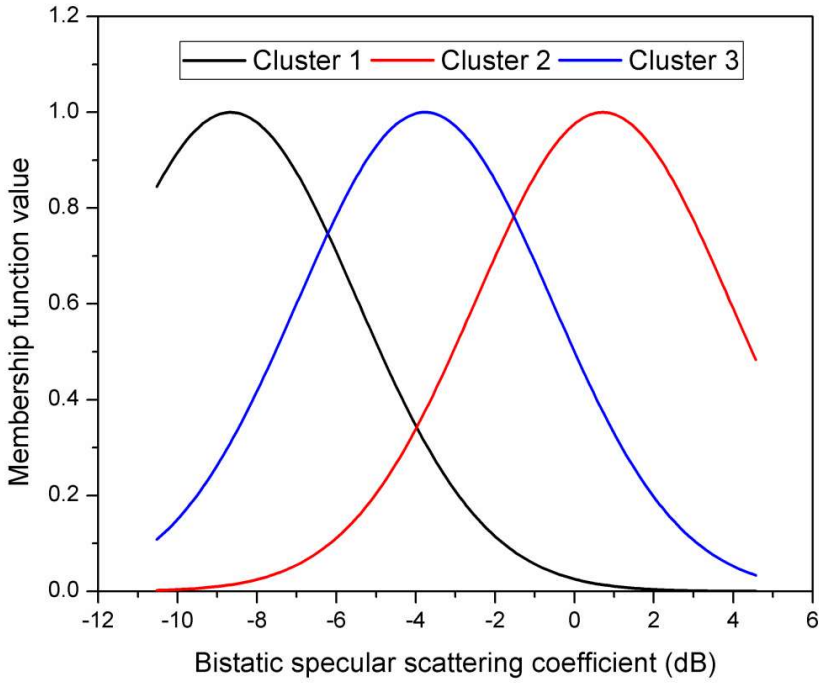

Figure 5.5 Membership function plot for FBm at X-band for VV-polarization

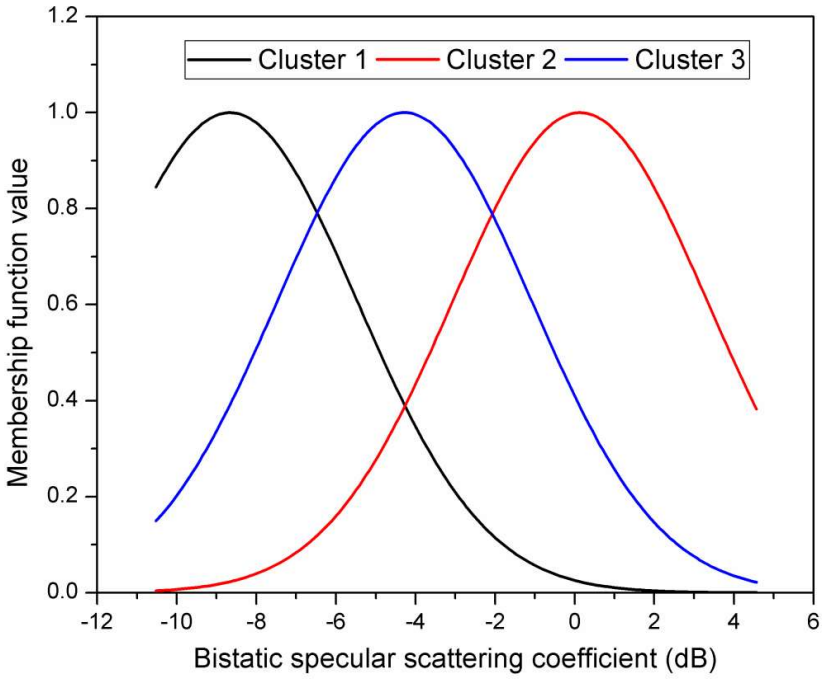

Figure 5.6 Membership function plot for LAI at X-band for VV-polarization

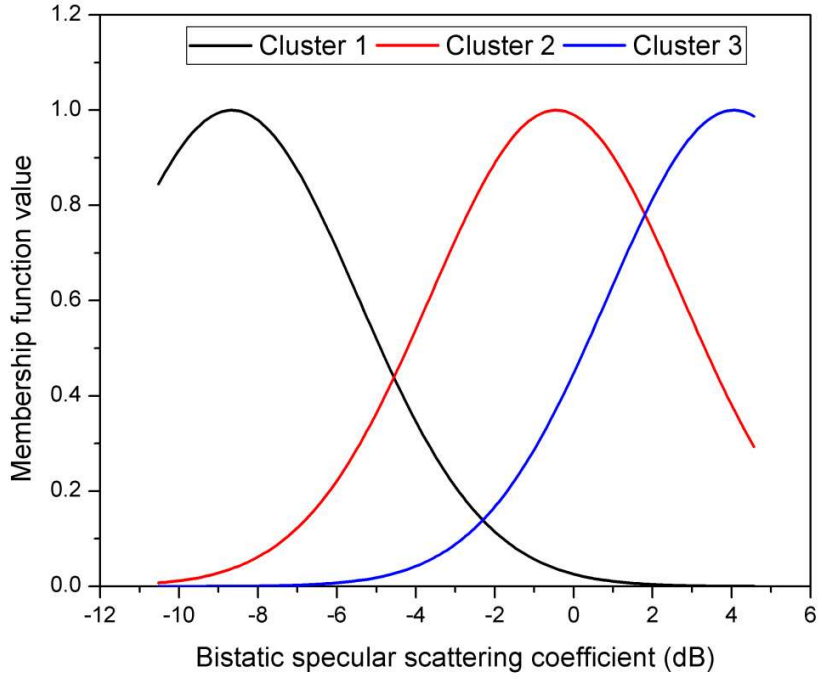

Figure 5.7 Membership function plot for PH at X-band for VV-polarization

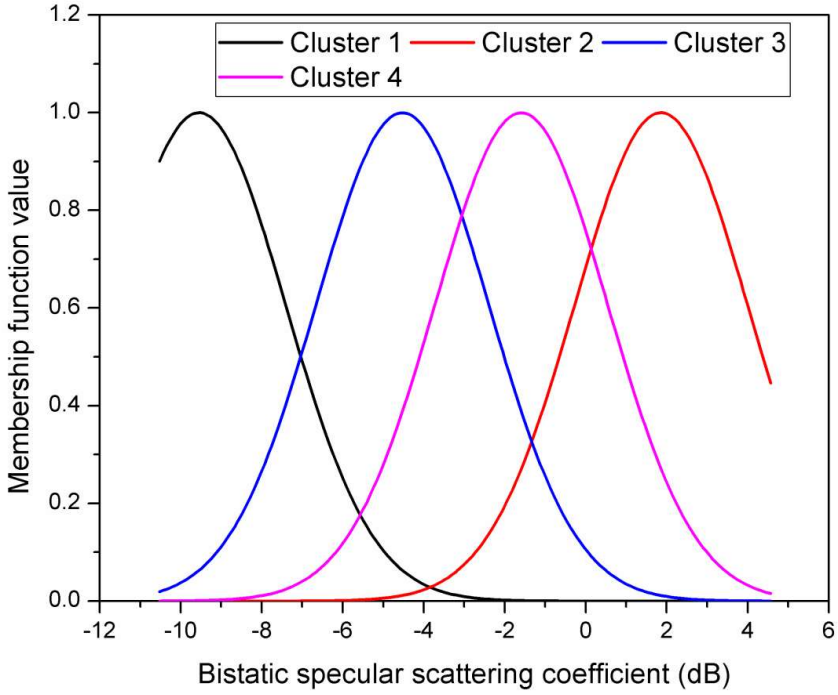

Figure 5.8 Membership function plot for VWC at X-band for VV-polarization

Table 5.2 Comparison of RMSE of S-FIS and S-ANFIS algorithm for different crop growth parameters

Crop growth parameters	S-FIS		S-ANFIS	
	RMSE (training)	RMSE (testing)	RMSE (training)	RMSE (testing)
FBm	0.0307	0.0384	0.0204	0.0280
LAI	0.0486	0.0658	0.0383	0.0556
PH	0.1707	0.1745	0.1617	0.1623
VWC	0.0233	0.0239	0.0121	0.0131

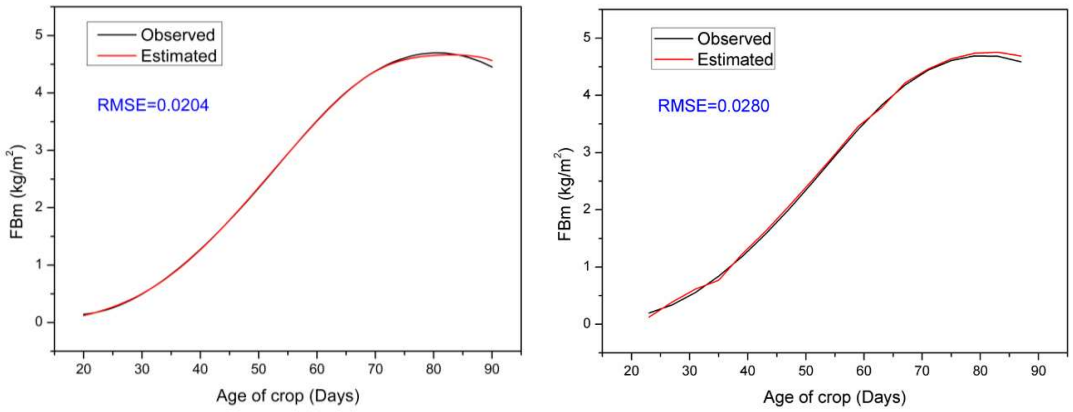

(a) **(b)**

Figure 5.9 S-ANFIS performance for the estimation of FBm at 40° angle of incidence for VV-polarization at X-band for (a) training and (b) testing

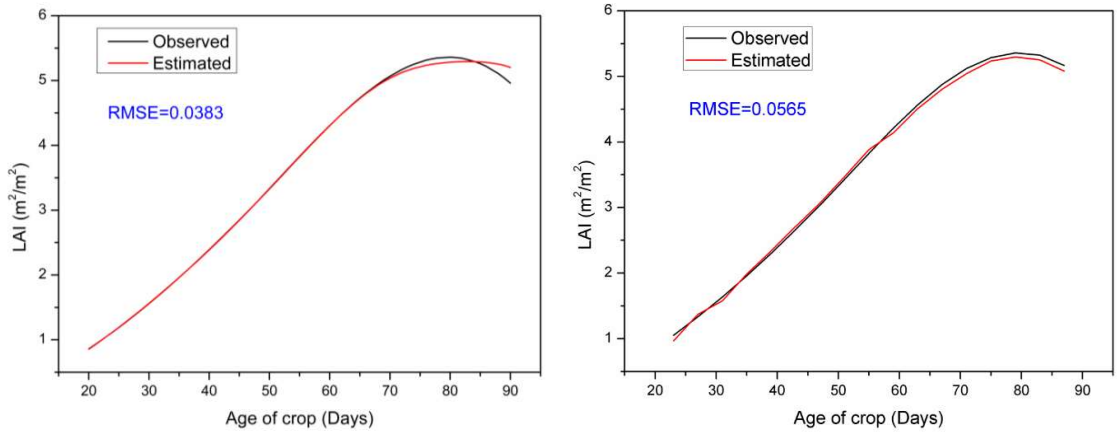

(a) **(b)**

Figure 5.10 S-ANFIS performance for the estimation of LAI at 40° angle of incidence for VV-polarization at X-band for (a) training and (b) testing

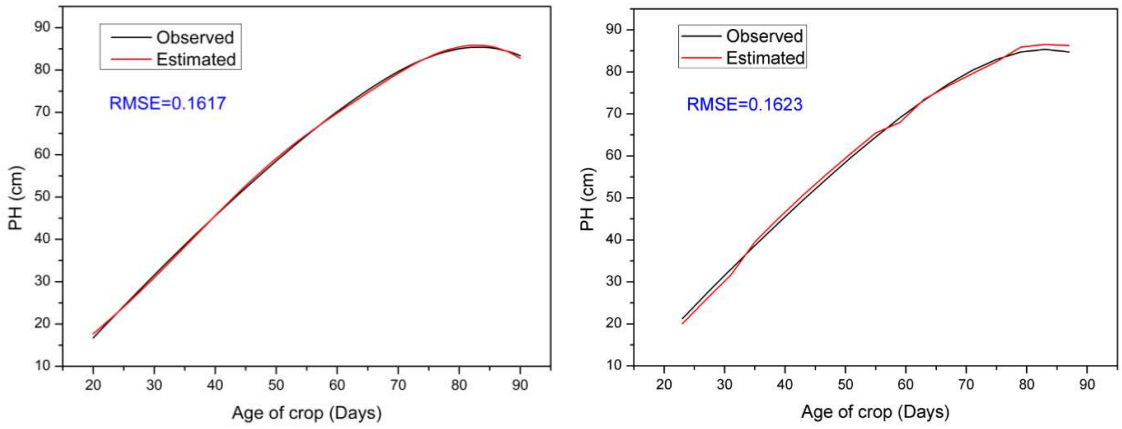

(a) **(b)**

Figure 5.11 S-ANFIS performance for the estimation of PH at 40° angle of incidence for VV-polarization at X-band for (a) training and (b) testing

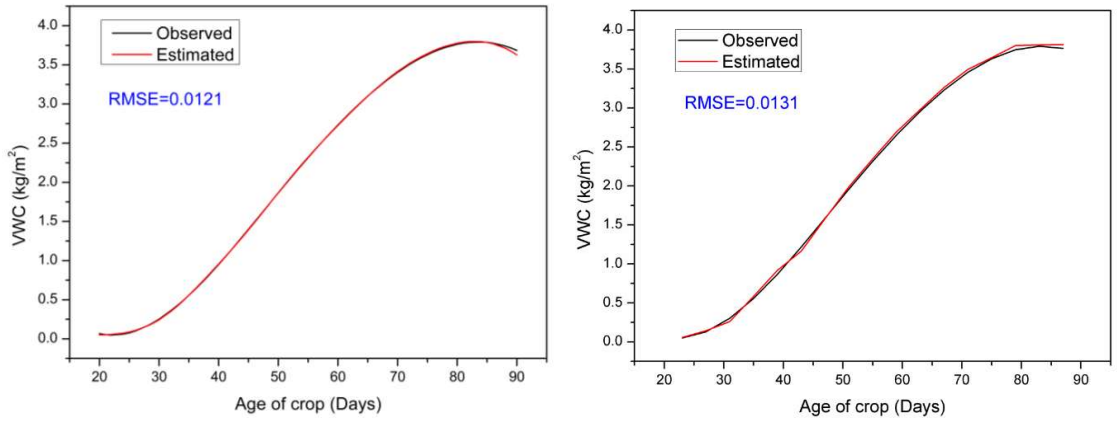

(a) **(b)**

Figure 5.12 S-ANFIS performance for the estimation of VWC at 40° angle of incidence for VV-polarization at X-band for (a) training and (b) testing

5.5 CONCLUSIONS

The crop growth variables, namely FBm, LAI, PH, and VWC, were found increasing until the maturity of the crop then started decreasing slightly. The decreasing trend of the specular bistatic scattering coefficient of ladyfinger crop was found with the age of crop and incidence angles till the maturity stage. After the maturity stage of the crop, the marginal increasing trend of specular bistatic scattering coefficients of ladyfinger crop was found with the age of the crop. The significant linear correlation was found between specular bistatic scattering coefficients and ladyfinger crop growth variables for the entire angular range of the incidence angles at both the polarizations. The highest value of coefficients of determination (R^2) was found between specular bistatic scattering coefficient and crop growth variables at 40^o incidence angle for VV- polarization. The potential of the S-ANFIS algorithm was found good during the testing for the estimation of crop growth variables at VV- polarization for the chosen optimum value of the cluster radius. The RMSE values between observed and estimated values of the crop parameters showed that the performance of the S-FIS was improved by using the S-FIS combined with the artificial neural network. Therefore, these results for the estimation of crop growth variables may be useful to suggest the suitable angle of incidence, polarization at X-band for the upcoming bistatic SAR mission for ladyfinger crop, as well as other agricultural crops having similar canopy structure.